High-Resolution 3-D Radar Imaging through Nonuniform Fast Fourier Transform (NUFFT)

Jiayu Song[1], Qing H. Liu[1,*], Kangwook Kim[2] and Waymond R. Scott, Jr.[2]

[1] *Department of Electrical and Computer Engineering, Duke University, Durham, NC 27708, USA.*

[2] *School of Electrical and Computer Engineering, Georgia Institute of Technology, Atlanta, GA 30332, USA.*

Abstract. This paper applies a 3-D nonuniform fast Fourier transform (NUFFT) migration method to image both free-space and buried targets from data collected by a ultra-wideband ground penetrating radar (GPR) system. The method incorporates the NUFFT algorithm into 3-D phase shift migration to evaluate the inverse Fourier transform more accurately and more efficiently than the conventional migration methods. Previously, the nonuniform nature of the wavenumber space required linear interpolation before the regular fast Fourier transform (FFT) could be applied. However, linear interpolation usually degrades the quality of reconstructed images. The NUFFT method mitigates such errors by using high-order spatial-varying kernels. The NUFFT migration method is utilized to reconstruct GPR images collected in laboratory. A plywood sheet in free space and a buried plexiglas chamber are successfully reconstructed. The results in 3-D visualization demonstrate the outstanding performance of the method to retrieve the geometry of the objects. Several buried landmines are also scanned and reconstructed using this method. Since the images resolve the features of the objects well, they can be utilized to assist the landmine discrimination.

1 Introduction

Ground-penetrating radar (GPR) is an ultra-wideband detecting technique used for subsurface exploration and monitoring. Many works have been done in the area of statistical signal processing to develop powerful statistical models to discriminate the targets [6, 8, 10]. On the other

---

*Correspondence to: Qing H. Liu, Department of Electrical and Computer Engineering, Duke University, Durham, NC 27708, USA. Email: `qhliu@ee.duke.edu`

hand, the abundant information carried by GPR data also provides a possibility to reconstruct high resolution images of the objects beyond just a confidence of detection. Three-dimensional image reconstruction from GPR data is therefore of great interest lately. Migration is one of the most useful time domain inversion methods as it focuses the reflections and diffractions to their actual positions. Various migration techniques have been studied to refocus the scattered signals from the time domain back to their true spatial locations in the object space. Kirchhoff depth migration [2–4], finite difference migration [16, 17] and phase-shift migration [9, 11] are the ones most widely used for seismic imaging. Recently, based on the seismic migration, Song and Liu [20] proposed a two-dimensional phase-shift migration method using nonuniform DFT for GPR landmine imaging and achieved promising results.

The migration methods usually migrate data in the frequency-wavenumber domain, therefore inverse Fourier transform is needed as a key step to transform the migrated data back to spatial domain. However, due to the nonuniform nature of the frequency-wavenumber space data, most of the migration methods share a common problem, i.e., the FFT is not directly applicable. This is because when data are not located on a uniform Cartesian grid, the multi-dimensional discrete Fourier transform can no longer be evaluated by the tensor product of multiple 1-D FFTs. Previous works used linear interpolation method [27] or direct summation method [20] to solve this problem. However, the interpolation-FFT method degrades the accuracy of discrete Fourier transform (DFT) and direct summation is computationally too expensive to evaluate.

The problem with the nonuniformly sampled data has been recently addressed by the nonuniform fast Fourier transform (NUFFT) algorithms [1, 7, 12–15, 26]. The direct evaluation of a nonuniform discrete Fourier transform (NUDFT) costs $\mathcal{O}(N^2)$ arithmetic operations, whereas the NUFFT algorithms reduce this to $\mathcal{O}(N \log N)$. The NUFFT algorithms have been applied to biomedical image reconstruction [18, 19, 23, 25], as well as to subsurface sensing for landmine detection and other buried objects [21, 22, 24].

Recently, several new data sets for complicated objects and landmines have been obtained by an ultra-wideband radar system developed at Georgia Institute of Technology. In this paper, an NUFFT-based image processing method based on the phase-shift migration [9, 20] is applied to process these data sets to achieve high resolution images. The nonuniform fast Fourier transform (NUFFT) algorithm proposed by Liu and Nguyen [13, 15] has been utilized to process the nonuniform discrete Fourier transform data. The NUFFT-based reconstruction method improves both accuracy and speed compared to the conventional phase-migration method. In section 2, the formulation and application are applied to 3-D objects. In section 4, the new 3-D NUFFT GPR migration method is applied to experimental data sets collected at Georgia Institute of Technology (section 3). The reconstructed results for a plywood sheet, a buried plexiglas chamber, and several landmines are excellent.

2 Theory

In subsurface sensing application of a GPR system, the transmitter sends out an electromagnetic wave to the ground. The transmitted signal traverses the ground surface and is scattered by
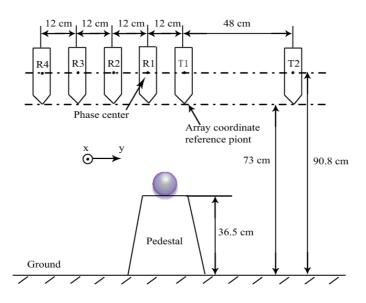
Figure 1: The 3-D multi-static GPR experiment setup for the free space target scan. The antennas are placed 73 cm from the surface of the ground and the targets are at a 36.5 cm height.

the target as well as the ground surface and potential heterogeneous soil. The scattered waves are then received by a receiving antenna, which is usually located in a close vicinity of the transmitting antenna. The ultra-wideband GPR we utilize here consists of two transmitting antennas and four receiving antennas, but only data from the two closest antennas are actually used. In Figs. 1 and 2, transmitter T1 and receiver R1 pair shows such a bistatic measurement setup where the object is located in the air or buried. If the mid-point between R1 and T1 antennas is denoted as (x, y, z) and is called the location of the GPR, the received signal for a wideband system can be denoted as $u(x, y, z, t)$ where t is time. The objective of GPR imaging is to reconstruct the induced source in the target that gives rise to this received signal.

Imaging the unknown target from the measured waveforms is an inverse problem. Among various inverse solutions, migration methods [5, 9] is a very attractive method because of their simplicity. The objective of migration methods is to refocus the scattered waves back to the actual spatial positions of the scatterers that give rise to such scattering. The phase shift method [9, 27] is utilized here for its simplicity and robustness. Among various migration methods [5], the phase-shift method can most easily incorporate the depth variation in wave velocity of the medium. The method is based on an exploding-reflector model with initial conditions defined by a zero-offset section (i.e., when the transmitter-receiver spacing is zero). Similar to the seismic migration method [9], the 3-D electromagnetic migration method utilized here was developed by assuming that only one electromagnetic field component is radiated and received so that it is reasonable to use a scalar wave equation; this is a reasonable simplification because in our measurements, we only used the co-polarized component in the transmitting and receiving antennas. Since the phase-shift migration method has been well documented in [5, 9], below we will only summarize the parts relevant to the NUFFT and its application.
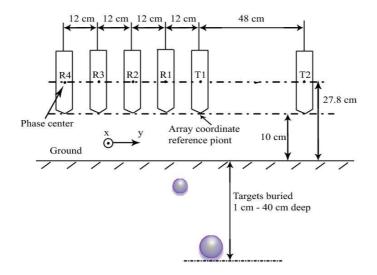
Figure 2: The 3-D multi-static GPR experiment setup for subsurface target scan. The antennas are placed 10 cm from the surface of the ground and the targets are buried at depths of 1 cm to 40 cm.

2.1   The NUFFT phase-shift migration

The measured waveform $u(x, y, z = 0, t)$ is obtained on a uniform spatial grid on the xy plane at $z = 0$ and is sampled uniformly in the temporal (t) direction. From $u(x, y, z = 0, t)$, the goal of a 3-D phase-shift migration method is to obtain the 3-D induced "source" at the scatterer, or $u(x, y, z, t = 0)$. To achieve this goal, the time-space domain (x, y, z, t) waveform $u(x, y, z, t)$ is transformed into the frequency-wavenumber domain (k_x, k_y, z, ω) through a regular 3-D Fourier transform (FT) to arrive at the transformed wave field $U(k_x, k_y, z, \omega)$. The original wave field $u(x, y, z, t)$ can be viewed as the plane-wave expansion of the transformed wave field. In this transformed domain, the plane wave propagates in the downward ($+z$) direction with a propagator $e^{ik_z z}$. Therefore, the transformed data $U(k_x, k_y, 0, \omega)$ can be downward continued with $e^{ik_z z}$ to obtain the corresponding data $U(k_x, k_y, z, \omega)$ at a depth z. From the 3-D inverse Fourier transform one can obtain the wave field at z as $u(x, y, z, t)$. Subsequently, by evaluating $u(x, y, z, t)$ at $t = 0$ where the scatterers are located, one obtains the 3-D induced "source" $u(x, y, z, t = 0)$. Consequently, starting from surface $z = 0$, the wavenumber-space data at an arbitrary depth can be obtained by this wave extrapolation. Mathematically, the migrated wavenumber-space data are transformed back to the spatial domain electromagnetic field $u(x, y, z, 0)$ using the inverse Fourier transform

$$u(x, y, z, 0) = \frac{1}{8\pi^3} \int \int \int U(k_x, k_y, 0, \omega) e^{i(k_x x + k_y y + k_z z)} dk_x dk_y d\omega \qquad (2.1)$$

where the wavenumbers k_x, k_y, k_z and frequency ω satisfy the dispersion relation

$$v^2(k_x^2 + k_y^2 + k_z^2) = \omega^2 \qquad (2.2)$$

and v is the wave speed in the medium. The discretization of (2.1) leads to

$$u(x_p, y_q, z_r, 0) = \frac{\Delta k_x \Delta k_y \Delta \omega}{8\pi^3} \sum_{j=0}^{J-1} \sum_{m=0}^{M-1} \sum_{n=0}^{N-1} U(k_x^j, k_y^m, 0, \omega^n) e^{i(k_x^j x_p + k_y^m y_q + k_z^n z_r)} \qquad (2.3)$$

where J, M, and N are the number of data points in x, y, and t directions, respectively, and (x_p, y_q, z_r) denotes the locations of uniform grid points for the 3-D image of the target.

As can be observed from equation (2.2), since the frequency and wave numbers are nonlinearly related with each other, at least one wavenumber dimension is nonuniform if the temporal discretization is uniform. As a result, the regular FFT cannot be directly applied. In practice, since the data are sampled uniformly on the ground surface and in time domain, k_x, k_y, and ω are equally spaced, thus the samples are then non-equally spaced along k_z. Linear interpolation is conventionally used to resample the nonuniform data onto a uniform grid. However, such linear interpolation usually introduces a significant approximation error. In this work, Liu and Nguyen's [13,15] NUFFT is integrated into the phase-shift migration to solve this problem. The NUFFT algorithm can efficiently evaluate the DFT. A weight matrix is computed by approximating the exponential of one node as a summation of exponentials of $q + 1$ nodes. The approximation error is minimized in a least square sense. With this migration algorithm, the discrete Fourier transforms along k_x and k_y directions in (2.3) can be accurately evaluated with the regular 2-D FFT while the one along k_z is computed by the NUFFT, i.e.,

$$u(x_p, y_q, z_r, 0) = \frac{\Delta k_x \Delta k_y \Delta \omega}{8\pi^3} [\text{FFT}_{k_x, k_y}][\text{NUFFT}_{k_z}]\{U(k_x^j, k_y^m, 0, \omega^n)\}. \qquad (2.4)$$

The advantage of using the NUFFT algorithm for the above migration are: (a) there is no need to perform linear interpolation of the data at different measurement sites, since the weight matrices are obtained for the exponential kernel rather than the data; (b) the accuracy is much higher as the NUFFT uses a much more accurate approximation.

2.2 The NUFFT algorithm

Here we summarize the NUFFT algorithm we used for this imaging application. For more details, the reader is referred to [13,15]. As is well known, the condition of using the regular FFT algorithm is that the data acquisition must be equispaced. However, as described above, although the data acquisition in our GPR sensing is uniformly spaced on the xy plane and along the temporal direction, it is not uniform in the k_z space because of the nonlinear dispersion relation (2.2). In [13,15], an accurate and efficient NUFFT algorithm was developed by using the regular Fourier matrices. In the NUFFT algorithm, the goal is to develop a fast algorithm to find the nonuniform discrete Fourier transform (NUDFT)

$$\tilde{h}_m = \frac{1}{\sqrt{N}} \sum_{n=0}^{N-1} h(t_n) e^{it_n m \frac{2\pi}{N}}, \quad t_n \in [0, N), \quad m = 0, \cdots, N-1 \qquad (2.5)$$

where for notation simplicity we identify t with the nonuniform wavenumber k_z in (2.3). Obviously, the direct summation of this NUDFT costs $\mathcal{O}(N^2)$.

The principle of using the regular Fourier matrices [13, 15] to solve (2.5) is as follows. Instead of interpolating the input data $\{h(t_n)\}$, we will interpolate the exponential function $\exp{(i2\pi tm/N)}$ for each $t = t_n$ $(n = 0, \cdots, N-1)$. We consider a discrete sequence

$$f(m) = s_m e^{i2\pi t_n m/N}, \quad m \in \{0, \cdots, N-1\}, \tag{2.6}$$

where $t_n \in [0, N)$ is real, q is an even positive integer, and the accuracy factors s_m, $0 \le s_m \le 1$ for $m = 0, \cdots, N-1$, are chosen to minimize the error. Denoting $w = e^{i\frac{2\pi}{\nu N}}$, we will now interpolate $f(m)$ using the exponential function at $q + 1$ points on a unit circle, i.e.,

$$s_m w^{m\nu t} = \sum_{k=-q/2}^{q/2} x_k(t) w^{m([\nu t]+k)}, \quad m = 0, \cdots, N-1, \tag{2.7}$$

where $[a]$ denotes the integer nearest to a, and $x_{-q/2}(t), \cdots, x_{q/2}(t)$ are some unknown interpolation coefficients to be determined.

It was shown in [13,15] that the unknown interpolation coefficients $x(t) = [x_{-q/2}(t), \cdots, x_{q/2}(t)]^T$ can be determined by the least-squares method

$$x(t) = F^{-1} y(t) \tag{2.8}$$

where for $j, k = 0, \cdots, q$ we have a closed-form solution for the regular Fourier matrix

$$F_{jk}(\nu, N, q) = \begin{cases} N, & j = k \\ \frac{w^{(j-k)N/2} - w^{(k-j)N/2}}{1 - w^{(k-j)}}, & j \ne k \end{cases} \tag{2.9}$$

It is observed that while $y(t)$ depends on t, matrix $F(p, N, q)$ is completely independent of t and is uniquely determined by ν, N and q. The matrix $F(\nu, N, q)$ is called the *regular Fourier matrix*; it is a $(q + 1) \times (q + 1)$ Hermitian matrix, $F(\nu, N, q)^\dagger = F(\nu, N, q)$.

If the scaling factors are chosen as the cosine functions $s_m = \cos\frac{\pi m}{\nu N}$ for $m = 0, \cdots, N-1$, vector $\{y_k\}$ can also be written in a closed form:

$$y_k(t) = \sum_{m=0}^{N-1} s_m w^{(\{\nu t\}+q/2-k)m} = i \sum_{\gamma=-1,1} \frac{\sin[\frac{\pi}{2\nu}(2k - \gamma - q - 2\{\nu t\})]}{1 - e^{i\frac{\pi}{\nu N}(2\{\nu t\}+q-2k+\gamma)}} \tag{2.10}$$

where $\{\nu t\} = \nu t - [\nu t]$.

The NUFFT algorithm consists of following steps:

  (i) Compute $y_k(t_n)$ by (2.10) for $k = 0, ..., q$ and $n = 0, \cdots, N-1$. The complexity is $\mathcal{O}(Nq)$.

  (ii) Compute $P_{jn} = \sum_{k=0}^{q} [F^{-1}]_{jk} y_k(t_n)$, where the inverse regular Fourier matrix F^{-1} is precomputed. The complexity is $\mathcal{O}(Nq^2)$.

(iii) Find the inverse of the scaling factor s_m^{-1}. For the cosine scaling factors $s_m^{-1} = \sec \frac{\pi m}{\nu N}$ for $m = 0, \cdots, N-1$. The complexity is $\mathcal{O}(N)$.

(iv) Calculate Fourier coefficients

$$\tau_l = \sum_{j,n,[\nu t_n]+j=l} h(t_n) \cdot P_{jn}.$$

The complexity is $\mathcal{O}(Nq)$.

(v) Use the regular uniform FFT to evaluate

$$T_m = \sum_{l=0}^{\nu N - 1} \tau_l \cdot e^{i2\pi ml/\nu N}.$$

The complexity is $\mathcal{O}(\nu N \log N)$.

(vi) With a complexity of $\mathcal{O}(N)$, scale the values to arrive at the approximated nonuniform FFT

$$\tilde{h}_m = T_m \cdot s_m^{-1}.$$

The total complexity is $\mathcal{O}(N \cdot q^2 + \nu N \log N)$, noting that $q \sim \log(1/\epsilon)$ where ϵ is the precision, and $\nu \ll N$ (usually $\nu = 2$).

Depending on the nonuniformity of the data, the NUFFT retains the accuracy of direct DFT with a relative error level of $10^{-6} \sim 10^{-12}$. Compared to the linear interpolation method, the NUFFT relative error is usually five orders of magnitude lower. Furthermore, the complexity for evaluating a sequence of length N approaches $\mathcal{O}(\nu N \log N)$, where ν is an oversampling rate. The pre-processing time to calculate the weight matrix has been reasonably excluded from the overall processing time since typically it remains unchanged for practical systems where the data acquisition configuration is fixed. This is much faster than the direct summation approach that requires $\mathcal{O}(N^2)$ operations.

3   Data acquisition

A multi-static GPR experiment has been performed at Georgia Institute of Technology with six ultra-wideband antennas. The configurations for the free-space experiment is illustrated in Fig. 1, while the configuration for buried objects is shown in Fig. 2. The antenna beams point toward the ground and the array lies along the y axis. A 192 cm-wide synthetic array aperture is obtained by using reciprocity and synthesizing the scans at 90 positions.

Data acquisition is performed on targets both in free space and underground. In these experiments, a square region of 180 cm × 180 cm is scanned with a sampling interval of 2 cm. The antennas operate in the frequency range of 60 MHz ∼ 8.06 GHz, with 401 equally spaced frequency sample points. From these frequency-domain data, the time-domain waveforms are obtained by the inverse FFT to arrive at 1024 equally spaced temporal sample points for each received signal before our 3-D NUFFT migration processing is performed.

As shown in Fig. 1, in the free space case, the antennas are placed 73 cm above the ground and the targets are at a height of 36.5 cm. The targets scanned in free space include several metal spheres, landmines, and a plywood sheet of the letters "GT". Fig. 2 shows the configuration to scan the buried targets. In this case, the antennas are 10 cm above the ground surface. A plexiglas chamber, a grid of metal spheres and landmines are buried under sand at depths varying from 1 cm to 40 cm. In both of the free-space and underground cases, datasets corresponding to the absence of targets are also acquired for calibration purpose.

4   Data processing

For the purpose of NUFFT migration, the wave field data acquired by the two closest antennas, i.e., transmitter 1 (T1) and receiver 1 (R1), are used, and denoted below as "raw data". The waveform recorded by this pair can be treated as the backscattered data, as assumed in the formulation. One advantage of the NUFFT migration is that it works well without much prior information about the medium. In contrast, to reconstruct buried targets, many other inversion methods require the prior information of soil electrical parameters such as conductivity, permittivity and permeability. However, this NUFFT migration method can process without any specific knowledge about the soil properties except the mean wave velocity through the two way path. We estimate this velocity by using the corresponding 2-D migration method as part of the preprocessing. Assuming that the subsurface wave velocity is generally the same over the entire 3-D volume, a 2-D xz slice is extracted for velocity estimation. The velocity is gradually changed from a lower value to the speed of light in vacuum, and the one with best focusing performance is selected. As a result, compared to many iterative inversion algorithms, this method is much simpler and faster.

The preprocessing of this migration method includes calibration, wave velocity estimation and calculation of the weight matrix in NUFFT given the measurement configuration. The calibration first removes artifacts from the free space measurements by zeroing out late-time signals, then normalizes using the through-calibration data obtained by directly transmitting the signal from the transmitter to the receiver in the absence of objects. After calibration, one 2-D xz slice containing the target signal is extracted from the 3-D dataset and a 2-D NUFFT migration is performed. The 2-D NUFFT migration method can be readily obtained from the formulation by fixing one horizontal dimension. An optimal estimate of wave velocity in the soil is decided while the migrated image of the target is best focused, as shown in Fig. 3. The 2-D processing is used because it can provide an accurate wave velocity estimate for the subsequent 3-D migration with little computation time. Both the calibration and velocity estimation are location dependent hence need to be done for each different target.

The weights matrix, however, does not need to be re-calculated as long as the experimental configuration remains the same. This is one of the key intrinsic advantages of using NUFFT algorithm versus other interpolation methods. With NUFFT, the speed of Fourier transform evaluation approaches the regular FFT (except for an oversampling factor of $\nu = 2$ in our calculation). In the GPR processing, since the experimental setups for all the targets in both
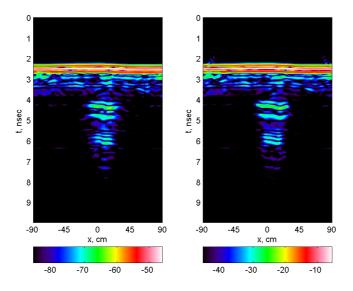
Figure 3: The 2-D processing of a xz slice to estimate the wave velocity in the soil. For the case of a buried chamber, the velocity is estimated to be $1.8 \times 10^8 m/s$. Left: The 2-D GPR raw data. Right: The 2-D NUFFT migrated data.

Figure 4: The 3-D isosurface of the reconstructed "GT" plywood.

free space and underground cases are the same, the weights matrices for all the reconstructions are identical and are pre-calculated. The GPR datasets are then processed by the 3-D NUFFT migration with the velocity estimated using the 2-D NUFFT migration method. Some of the migrated results are listed in the next section, including a plywood sheet in free space, a plexiglas chamber and a grid of landmines buried under sand.

Table 1: The estimated dimensions of the "GT" plywood and the relative estimation errors compared to the ground truth.

Size	Ground Truth	Estimation	Relative Error (%)
Width	38.5 cm	38 cm	1.30%
Height	46.5 cm	44 cm	5.38%
Thickness	1.8 cm	1.76 cm	2.22%

5 Results

3-D images are obtained by the NUFFT migration of array waveforms collected at the 2-D array parallel to the ground surface. Horizontal slices at specified depths are good presentations of the 3-D migration results. Below the raw data and the images obtained by migration are listed together for comparison.

5.1 Case 1: The GT plywood

A plywood sheet is carved into a relatively complicated shape consisting of two letters "G" and "T". The plywood is 38.5 cm wide, 46.5 cm high, and 1.8 cm thick, and lies on a horizontal plane parallel to the ground surface. The complicated shape and small thickness pose significant challenges for accurate reconstruction. The magnitudes of the inverted wave field as well as the raw data are plotted as gray scale images and shown in Fig. 5. The reconstructed "GT" sign (right) using NUFFT migration is very close to the true target and the complicated details are well resolved. It is certainly much better than the image of raw data (left). The raw image suffers from the overlapping diffraction hyperbolae in the received GPR waveforms, while the NUFFT-migration method collapses those hyperbola to their diffraction apices, thus uncovering the true 3-D image of the target. The horizontal slice suggests good contrast on the boundary of the reconstructed image so that the target can be clearly differentiated from the background. A 3-D visualization of the "GT" plywood generated using an isosurface is provided in Fig. 4 to further demonstrate that the method is capable of reconstructing the high-resolution target geometry. The isovalue selected to produce the 3-D view is 0.5226 relative to the maximum. Actually, the dimensions of the plywood sheet can be estimated quantitatively using the migrated 3-D image. The estimated object is 38 cm wide, 44 cm high, and 1.76 cm thick. The horizontal spatial resolution is 2 cm in each of the two dimensions and the vertical spatial resolution is 0.29 cm. The relative estimation errors of this "GT" plywood geometry are listed in Table 1.

5.2 Case 2: A buried plexiglas chamber

A chamber made of 2.54 cm-thick plexiglas is buried in a sand pit at a depth of 9.5 cm from the top of the chamber. The exterior dimensions of the chamber are 40.64 cm × 30.48 cm × 20.32 cm. Based on the 2-D migrated results, a wave velocity of 1.8×10^8 m/s is utilized for the sand in the 3-D processing. The horizontal slices at the depths of 12 cm (near the upper

Table 2: The estimated dimensions of the buried plexiglas chamber and the relative estimation errors compared to the ground truth.

Size	Ground Truth	Estimation	Relative Error (%)
Width	40.64 cm	42 cm	3.35%
Height	30.48 cm	34 cm	11.55%
Thickness	20.32 cm	16.1 cm	20.77%
Depth	9.5 cm	10.5 cm	10.53%

Figure 5: The horizontal slice of the raw image and the 3-D migration reconstructed image of the GT plywood in free space. Left: The GPR raw data. Right: 3-D NUFFT migrated data at the plywood surface. The estimated size is 38 cm wide, 44 cm high and 1.76 cm thick.

chamber's surface) and 17 cm (around the middle of the chamber) from the ground surface are shown in Figs. 6 and 7. Because of the ground surface reflections and interference of the soil, as expected, the reconstructions are not as good as the above free space case. In particular, the image resolution is limited by the relatively low signal-to-noise ratio of the sensor data and the velocity estimation error as the soil is never strictly homogeneous. However, compared to the raw images, this NUFFT migration method significantly enhances the detection of the object and the identification of the geometry. The NUFFT migrated result of the chamber provides an estimation of 42 cm in width, 34 cm in length, and 16.1 cm in height, and the relative errors are given in Table 2.
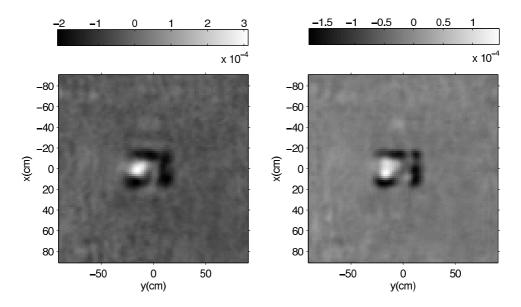
Figure 6: The horizontal slice of the raw image (left) and the 3-D migration reconstructed image (right) of the plexiglas chamber at a depth of 12 cm.
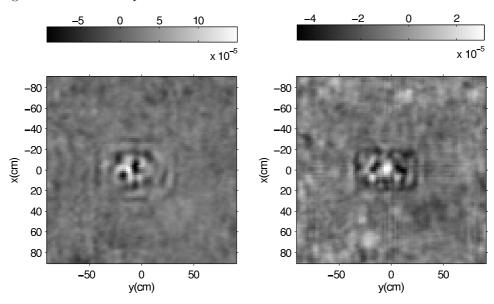

Figure 7: The horizontal slice of the raw image (left) and the 3-D migration reconstructed image (right) of the plexiglas chamber at a depth of 17 cm. The estimated size is 42 cm in width, 34 cm in length, and 16.1 cm in height.

5.3   Case 3: A grid of mines and clutters

Finally, a grid of several landmines and rock clutters are buried at different depths. The mines include M14, TMA-5, TS-50, PFM 1, VS 1.6, and VS 2.2, and the clutters are metal spheres,
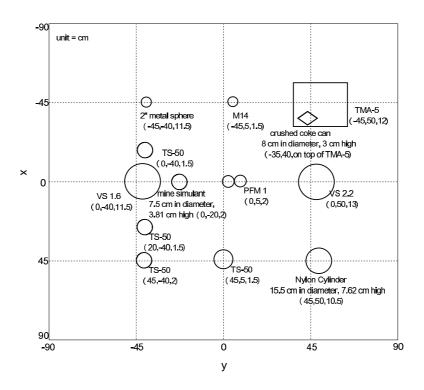
Figure 8: The buried map and sizes of the testing landmines.

rocks and a Nylon cylinder of various dimensions. The reconstructions at two depths (4 cm and 17 cm) in Figs. 9 and 10 are compared with the actual depths and sizes of the mines in Fig. 8. Both positions and geometries of TMA-5, VS 1.6 and VS 2.2 landmines are well reconstructed, but mines of smaller sizes are much more difficult to reconstruct. Although these reconstructed images alone may not be sufficient to accurately classify between mines and clutters, the focused energy and coarse geometry information will be very useful information for improving the discrimination based on the target features. Therefore, the NUFFT migration method can be further integrated with existing statistical classification techniques to improve the detection performance. A 3-D visualization of the VS 2.2 landmine buried at a depth of 13 cm is compared to the real geometry of the mine in Fig. 11. The isovalue selected for the 3-D view is 0.3200 relative to the maximum intensity value.

5.4   The processing speed

Besides its accuracy, the fast processing speed and the simplicity are also the advantages of the NUFFT migration method. With the weights matrix pre-computed, a 2-D slice can be processed within 0.2 second and the 3-D processing time for a dataset of $1024 \times 91 \times 91$ size is around 40 seconds. The fast evaluation of NUFFT enhances the speed of the overall migration processing. Given the GPR acquisition of a 3-D object usually takes around one minute, the
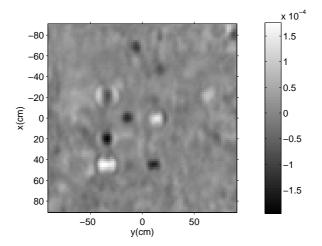
Figure 9: The horizontal slice of landmine image at a depth of 4 cm. The four buried TS-50 mines centered at $(-20, -40, 1.5)$ cm, $(20, -40, 1.5)$ cm, $(45, -40, 2)$ cm and $(45, 5, 1.5)$ cm, the mine stimulant at $(0, -20, 2)$ cm and two PFM-1 at $(0, 5, 2)$ cm can be observed on the reconstructed image.
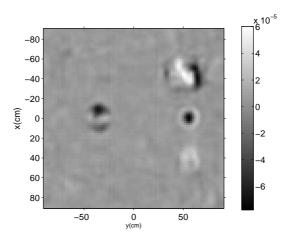

Figure 10: The horizontal slice of landmine image at a depth of 17 cm. The buried TMA-5 centered at $(-45, -50, 12)$ cm, the VS 2.2 at $(0, 50, 13)$ cm, the Nylon cylinder at $(45, 50, 10.5)$ cm, and the VS 1.6 at $(0, -40, 11.5)$ cm can be observed on the reconstructed image.

NUFFT migration method can finish the processing of one dataset within the acquisition time of next dataset. This makes the real time 3-D GPR imaging very promising.
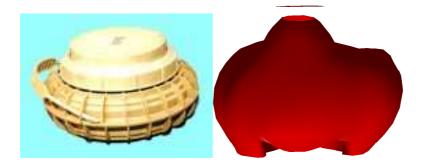
Figure 11: The actual (left) landmine VS 2.2 and its reconstructed 3-D isosurface. The landmine has a diameter of 24.0 cm and a height of 12.0 cm.

6 Conclusions

A 3-D NUFFT migration method has been applied for GPR image reconstruction. With the help of NUFFT, the Fourier transform of nonuniform frequency-wavenumber space samples can be evaluated efficiently and accurately. The method is demonstrated on several ultra-wideband GPR data collected in laboratory with multi-static experiments. It successfully reconstructs the 3-D geometries of several targets in both free space and buried underground. The estimated object sizes are very close to the ground truth. The method is simple, robust and efficient. Only a little background information is needed for the reconstruction. The processing speed is approximately the same as that of FFT because the latter include data interpolation, but NUFFT has an accuracy several times higher based on our synthetic image reconstruction. Thus, the NUFFT migration method is promising for real time GPR imaging of subsurface objects. The application on landmine, in particular, suggests that it can significantly improve the feature information from the raw data. It is hence very helpful to the mine detection if incorporated with existing statistical demining models.

Acknowledgments

References

[1] G. Beylkin, On the fast Fourier transform of functions with singularities, Appl. Comput. Harmonic Anal., 2 (1995), 363–382.
[2] G. Blacquiere, H. W. J. Debeye, C. P. A. Wapenaar and A. J. Berkhout, 3-D table-driven migration, Geophys. Prosp., 37 (1989), 925-958.
[3] J. Cabrera, W. Perkins, T. Hagen, D. W. Ratcliffe and W. Lynn, 3-D prestack depth migration: Implementation and case history, Soc. Expl. Geophys., Expanded Abstracts, 11 (1992), 948-951.

[4] J. Cao, A practical implementation of the multi-processing 3-D Kirchhoff prestack migration scheme on the Cray YMP systems, 54rd Mtg. Eur. Assoc. Expl. Geophys., Abstracts, (1992), 284-285.

[5] J. F. Claerbout, Imaging Earth's Interior, Blackwell Sci. Pub., Oxford, 1985.

[6] L. M. Collins, P. Gao and L. Carin, An improved Bayesian decision theoretic approach for land mine detection, IEEE T. Geosci. Remote Sensing, 37(2) (1999), 811-819.

[7] A. Dutt and V. Rokhlin, Fast Fourier transforms for nonequispaced data, SIAM J. Sci. Comput., 14(6) (1993), 1368-1393.

[8] P. D. Gader, M. Mystkowski and Y. Zhao, Landmine detection with ground penetrating radar using hidden Markov models, IEEE T. Geosci. Remote Sensing, 39(6) (2001), 1131-1144.

[9] J. Gazdag, Wave equation migration with the phase shift method, Geophysics, 43 (1978), 1342-1351.

[10] A. H. Gunatilaka and B. A. Baertlein, Subspace decomposition technique to improve GPR imaging of antipersonnel mines, in: A. C. Debey, J. F. Harrey, J. T. Broach and R. E. Dugan (Eds.), Proceedings of SPIE, vol. 4038, 2000, pp. 1008-1018.

[11] S. Lee, G. McMechan and C. Aiken, Phase-field imaging: The electromagnetic equivalent of seismic migration, Geophysics, 52 (1987), 678-693.

[12] Q. H. Liu, Fast Fourier Transforms and NUFFT, in: K. Chang (Ed.), Encyclopedia of RF and Microwave Engineering, Wiley-Interscience, 2005, pp. 1401-1418.

[13] Q. H. Liu and N. Nguyen, An accurate algorithm for nonuniform fast Fourier transform (NUFFT's), IEEE Microw. Guided Wave Lett., 8 (1998), 18-20.

[14] Q. H. Liu and X. Y. Tang, Iterative algorithm for nonuniform inverse fast Fourier transform (NU-IFFT), Electron. Lett., 34(20) (1998), 1913–1914.

[15] N. Nguyen and Q. H. Liu, The regular Fourier matrices and nonuniform fast Fourier transforms, SIAM J. Sci. Comput., 21(1) (1999), 283-293.

[16] J. Rickett, J. Claerbout and S. Fomel, Implicit 3-D depth migration by wavefield extrapolation with helical boundary conditions, Soc. Expl. Geophys., Expanded Abstracts, 17 (1998), 1124-1127.

[17] D. Ristow and T. Ruhl, Fourier finite-difference migration, Geophysics, 59(12) (1994), 1882-1893.

[18] G. Sarty, R. Bennett and R. Cox, Direct reconstruction of non-Cartesian k-space data using a nonuniform fast Fourier transform, Magn. Reson. Med., 45 (2001), 908-915.

[19] L. Sha, H. Guo and A. W. Song, An improved gridding method for spiral MRI using nonuniform fast Fourier transform, J. Magn. Reson., 162 (2003), 250-258.

[20] L. Song and Q. H. Liu, Ground-penetrating radar land mine imaging: Two-dimensional seismic migration and three-dimensional inverse scattering in layered media, Radio Sci., in press.

[21] J. Song and Q. H. Liu, 2D nonuniform fast Fourier transform (NUFFT) method for synthetic aperture radar and ground penetrating radar signal processing, 2004 URSI Meeting Abstract, Monterey, CA, June 2004.

[22] J. Song and Q. H. Liu, 3D non-uniform fast Fourier transform (NUFFT) based migration for subsurface object imaging, 2005 URSI Meeting Abstract, Washington, DC, July 2005.

[23] J. Song and Q. H. Liu, A novel medical ultrasound image reconstruction method through migration, 2005 URSI Meeting Abstract, Washington, DC, July 2005.

[24] J. Song, Q. H. Liu, P. Torrione and L. Collins, 2-D and 3-D NUFFT migration method for landmine detection using ground-penetrating radar, IEEE T. Geosci. Remote Sensing, submitted, 2005.

[25] B. Sutton, J. Fessler and D. Noll, A min-max approach to the nonuniform N-dimensional FFT for rapid iterative reconstruction of MR images, Proc. Int. Soc. Magn. Reson. Med., 9 (2001), 763.

[26] A. F. Ware, Fast approximate Fourier transforms for irregularly spaced data, SIAM Rev., 40 (1998), 838-856.

[27] O. Yilmaz and S. M. Doherty (Eds.), Seismic Data Analysis: Processing, Inversion, and Interpretation of Seismic Data, Society of Exploration Geophysicists, Tulsa, 2001.